Generalized approach for multi-response machining process optimization using machine learning and evolutionary algorithms

Tamal Ghosh*, Kristian Martinsen

Department of Manufacturing and Civil Engineering, Norwegian University of Science and Technology, Teknologivegen 22, 2815 Gjøvik, Norway

ABSTRACT

Contemporary manufacturing processes are substantially complex due to the involvement of a sizable number of correlated process variables. Uncovering the correlations among these variables would be the most demanding task in this scenario, which require exclusive tools and techniques. Data-driven surrogate-assisted optimization is an ideal modeling approach, which eliminates the necessity of resource driven mathematical or simulation paradigms for the manufacturing process optimization. In this paper, a data-driven evolutionary algorithm is introduced, which is based on the improved Non-dominated Sorting Genetic Algorithm (NSGA-III). For objective approximation, the Gaussian Kernel Regression is selected. The multi-response manufacturing process data are employed to train this model. The proposed data-driven approach is generic, which could be evaluated for any type of manufacturing process. In order to verify the proposed methodology, a comprehensive number of cases are considered from the past literature. The proposed data-driven NSGA-III is compared with the Multi-Objective Evolutionary Algorithm based on Decomposition (MOEA/D) and shown to attain improved solutions within the imposed boundary conditions. Both the algorithms are shown to perform well using statistical analysis. The obtained results could be utilized to improve the machining conditions and performances. The novelty of this research is twofold, first, the surrogate-assisted NSGA III is implemented and second, the proposed approach is adopted for the multi-response manufacturing process optimization.

1. Introduction

Recent Manufacturing Process Optimization Problems (MPOP) are challenging since these are complex, constrained, non-convex, multi-response, and dependent on many process variables (dependent and independent). Developing optimal, correlational, or functional models for MPOP would be the most demanding task. It is not easy to obtain optimized conditions for the MPOP since many design variables are involved, which are to be correctly selected for the improved responses. Due to the nonlinear relationships among the dependent and independent process variables, complicated design space is required for the MPOP, which makes the process more difficult to frame using mathematics or simulation [1]. Accuracy of certain machining processes are subject to the expensive experimental machining data, which is directly or indirectly connected with the machining costs, tool cost, labor costs, overhead costs, and scrap costs etc. Therefore, the data driven models, machine-learning techniques, meta-model or deep-learning approaches could be appropriate in such scenarios [2].

Since late 90s, Multi-Objective Evolutionary Algorithms (MOEAs) have been an evolving topic of research for solving real-world combinatorial problems [3,4]. These problems do not always portray process specific mathematical or simulation framework, which are computationally expensive. Empirical data obtained from laboratorial experiments or expensive simulations are employed to evaluate performance characteristics for such problems. MPOP is classified as data-driven or surrogate-assisted optimization problems [5].

When MOEAs are employed to solve the MPOPs, data-driven surrogate models are generally used as the objective functions, which potentially eradicates the need of performing computationally complex mathematical model, Finite Element Method (FEM) approach, or expensive empirical experiments [6,7]. It often facilitates the use of the traditional or existing optimization algorithms, such as, exact methods, evolutionary algorithms, and bio-inspired techniques as the optimal solution searching components. Surrogate modeling could also be classified as the black-box modeling when there would be little or no information available about the machining process under consideration [8]. Data-driven surrogate modeling approaches are capable of approximating functional relationships among the process variables based on the sampled data obtained using Design of Experiment (DOE) techniques [9]. Accuracy of the solution approximation would be crucial while training the models. For that matter Mean Square Error (MSE), Root Mean Square Error (RMSE), Normalized Mean Square Error (NMSE) could be used as the performance measures for the models. The lower is the performance measure score, the better is the accuracy of the model. Once the surrogate model is trained, an appropriate optimization algorithm, e.g. Genetic Algorithms (GA), Particle Swarm Optimization (PSO), Ant Colony Optimization (ACO), and Bat Inspired Algorithm (BA), Teaching-Learning Based Optimization (TLBO), Reference Vector Guided Evolutionary Algorithm (RVEA), Pareto Efficient Global Optimization (ParEGO) etc. could be employed to find good solutions, which would be the global (Pareto) optimum [10]. The data-driven surrogate models are substantially prompt and efficient; therefore, these are computationally inexpensive. DOE based tools, such as the central composite design (CCD), Box-Behnken De-sign (BBD), D-Optimal Design (DOD), Latin Hypercube Sampling (LHS), Full Factorial Design (FFD), and Orthogonal Array Design (OA) etc. are generally used to define the trial sample points as the initial population for the surrogate-assisted MOEAs. DOE methods are also used as the input data to the trained surrogate models. DOE methods generally maximize the process information obtained from the restricted number of trials [11]. Depending on the applications, some of the approximation approaches have become popular and practiced in recent past. These are, Response Surface Methods (RSM), Gaussian process (GP), Redial Basis Functions (RBF), Support Vector Machines (SVM), Multi-Layer Perceptron (MLP), Gaussian Kernel Regression (GKR), Artificial Neural Network (ANN), Generalized Regression Neural Network (GRNN) etc. [12].

* Corresponding author. Tel.: +47-909-12-002
e-mail: tamal.ghosh@ntnu.no

In this paper a novel data-driven surrogate-assisted optimization approach is introduced, which is based on the improved Non-dominated Sorting Genetic Algorithm (NSGA-III) and Multi-objective Evolutionary Algorithm based on Decomposition (MOEA/D). The proposed technique is developed using the data-driven surrogate function. Gaussian Kernel Regression (GKR) is used as the surrogate function. Further eleven published case studies of real-world MPOPs are employed to validate the proposed approach. The rest of this paper is structured as follows; Section #2 provides a detailed review of the recent literature; Section #3 demonstrates the proposed multi-response data-driven surrogate-assisted optimization; Section #4 presents the results and analyses; Section #5 concludes this work.

2. Literature Review

The classical MOEA is an iterative procedure, which starts with a randomly generated population of solutions initially. It evolves in each iteration using two genetic operators, known as crossover and mutation, in search of the Pareto solutions. The quality of the obtained solutions is evaluated by some suitable objective functions. Depending on the quality of the solutions, the offspring (new solutions) are selected (using selection operator) and passed on to the next iteration while converging towards optimality. For the data-driven MOEA, the empirical data or process knowledge are obtained from the manufacturing processes and used in the MOEA framework to improve the convergence speed and performance (Figure 1).

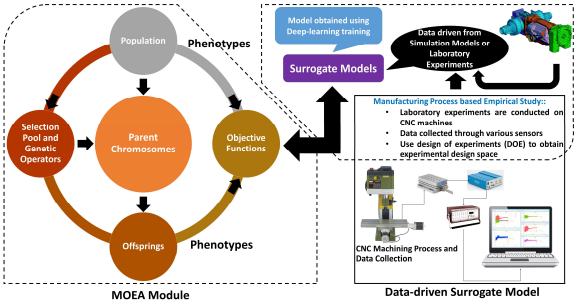

Figure 1. Data-Driven MOEA Framework

This in turn generates the optimal cutting conditions for the machining. Graning et al. [13] portrayed some complex large-scale real-world problem, which utilizes historical data to guide the search. Ref. Jin [14] demonstrated knowledge integration with evolutionary search, which is a process of information recycle obtained in past. Wang et al. [5] recently categorized the data-driven surrogate-assisted optimization based on the off-line and on-line modes. In off-line mode, no new data would be available during the optimization process. Therefore, the surrogate modeling is solely dependent on the empirical process data or simulation results obtained beforehand. Whereas, in on-line mode, new incremental data could be generated and added to the surrogate control during the optimization. The MPOP is considered as the former type. According to Guo et al. [15] these types of data-driven optimization approaches would be extremely challenging since the amount of data could be small with large approximation errors. Therefore, the obtained solutions could possibly be deviated from the actual values. This phenomenon suggests some validations or confirmatory tests on the solutions obtained [16].

2.1. Multi-Response Machining Processes

Most of the MPOPs are related to the manufacture of works in progress (WIP), semi-assemblies, which include multiple process variables (design parameters and performance characteristics). Therefore, multi-response optimisation plays a crucial role for the process quality improvement [17]. Selection of optimal process parameters inexpensively is a challenge. Over the decades, the tools and techniques for the multi-response MPOPs have been evolved considerably. Mukherjee and Ray [18] presented a comprehensive study on the methodologies developed for the multi-response MPOPs. Further, Chandrasekaran et al. [19] reviewed 142 articles based on the soft-computing and machine learning techniques for the multi-response MPOPs. Authors stated that, despite using the ANN or EA based techniques few more improvements are expected in future based on the costs involved in the data acquisitions, filtration of noise in data, and statistical feature extraction from the data. Figure 2 depicts a taxonomic classification based on the optimization techniques, which could be used in this regard.

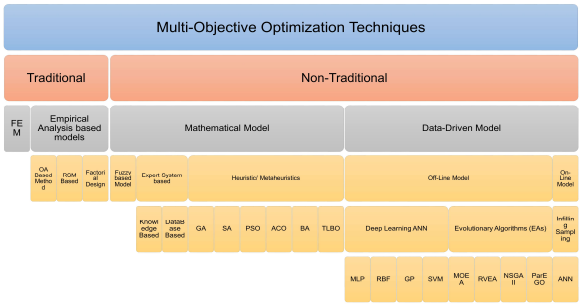

Figure 2. Taxonomical Classifications of Multi-Objective optimization techniques

The scope of this paper is limited to the off-line data-driven evolutionary algorithms. Various tools and techniques are being exploited for the data-driven MPOPs since decades. Cook et al. [20] have introduced an ANN based approximation model for particleboard manufacturing process. Authors then utilized a GA based algorithm to optimize the process parameters. Yarlagadda [21] proposed an ANN model to approximate the process parameters for the pressurized die casting process. This is an alternative way to replace the expensive experimental approach to obtain the process parameters by examining a physical model of the pressurized die casting process. Tabu Search (TS) and Simulated Annealing (SA) based approaches could also be found in literature [22-24]. Vijayakumar et al. [25] proposed an ACO for the multi-pass turning, which determines the machining parameters and minimizes the unit production cost, while considering various process constraints. Shen et al. [26] introduced a back propagation ANN model to correlate the complex process conditions and quality indexes for the injection molding process, and a GA is coupled to optimize the process conditions successfully. Zhou and Turng [27] developed a special data-driven model using GP for injection molding optimization. Thereafter, a hybrid GA is utilized to evaluate the model, which could yield the global optimal solutions within a pre-defined number of iterations. Ciurana et al. [28] proposed the modeling and optimization of the process parameters in pulsed laser based micromachining using the ANN and Multi-Objective PSO (MOPSO) to obtain better surface roughness and minimum volume errors. Zhao et al. [29] introduced a fast strip analysis as a surrogate model for the optimisation of an injection molding process. Further a PSO based algorithm is employed, which effectively optimize the process parameters. Kadirgama et al. [30] proposed an ACO based technique to obtain the optimum surface roughness for milling operation. The proposed technique exploited the RSM as a surrogate function. The most crucial variables are determined as the cutting speed, feed rate, axial depth, and radial depth. Shi et al. [31] have also developed an approximation model for injection molding process using the ANN and DOE. Authors introduced the infilling sampling, which could improve the global search. Therefore, it is an on-line data-driven optimization, which adds new samples while learning from the observed data. Dereli et al. [32] introduced some system tool based GA to optimize the process parameters for the prismatic parts. The tool is used as a standalone software for the process planning system. Thombansen et al. [33] introduced self-optimisation based on the self-adaptive machines, which shows intelligent reasoning abilities. Authors demonstrated an

automatic parameters adaptation by machines while dealing with the uncertainty. Farahnakian et al. [34] experimented with a statistical tool, ANN, and PSO algorithm to optimize the data obtained from the nanoclay content on PA-6 with reduced cutting forces. The results show that the satisfactory modeling of the cutting forces and surface roughness. Yusup [35] have portrayed a detailed survey on the EAs and Bio-Inspired techniques based applications for parametric designs of the machining processes during 2007 to 2011. Authors concluded that the GA based optimization approaches are heavily exploited and surface roughness is the most explored performance criterion during that period. Šibalija and Majstorovic [36] developed a three-stage expert system based on the design space planning using the OA, data processing using the factor effects approach and optimization using the ANN and EAs. Authors presented four case studies based on the non-conventional processes. Shakeri et al. [37] portrayed a regression based process model and ANN based predictive model for the Wire Electro-Discharge Machining (WEDM) to obtain better surface Roughness (Ra) and Material Removal Rate (MRR). Process variables considered are, pulse current, frequency of pulse, wire and servo speed. The ANN based method shows better performance. Arnaiz-González et al. [38] demonstrated the ball-end milling process models using the MLP and RBF, where RBF outperformed the MLPs. Xiang and Zhang [39] depicted a prediction model based on the ANN and SVM for the milling process modeling and proposed an optimization technique using the SVM and NSGA II. Zhou et al. [40] proposed an integrated multi-response technique based on the Grey Relational Analysis (GRA), RBF, and PSO for ball end milling. While compared with the classical GRA, it produces continuous space for optimality. Authors considered several design variables such as the inclination angle, cutting speed, feed, surface roughness, and compressive residuals stress. Khorasani and Yazdi [41] proposed some surface roughness monitoring system for the milling process considering the cutting speed, rate of feed, cut depth, type of materials, and coolant fluid, mechanical vibrations, white noise, and Ra. Thereafter testing and recall/verification procedures are utilized to achieve the higher accuracy. Sangwan and Kant [42] demonstrated an RSM based predictive model for the turning operation and optimize the model using GA. The results show that the depth of cut is the most influential parameter. D'Addona et al. [43] developed an application of ANN and DNA-based computing (DBC) to model the tool-wear. Tool-wear images are processed as data to train the ANN. The DBC can distinguish the image similarity or dissimilarity. Recent research trend shows that ANN based methods are very popular and useful as predictive models and being used heavily by the researchers. However, very few studies are proposed on the development of the surrogate models that can be used as a replacement of the empirical or mathematical functions for optimization. Pfrommer et al. [10] recently introduced a surrogate-based optimisation to a composite textile draping process, which is a deep ANN and it could predict the shear angle of a large number of textile elements. It is shown to minimize the number of FEM simulations to attain the optimum parameters. From the above discussion some interesting facts could be pointed out and the direction of this research could be determined,

- Data-driven optimization is an important area to be explored more for the MPOPs due to its capability to obtain the Pareto solutions [2].
- Most of the multi-objective research works considered two to four objectives, whereas more than four objectives are rarely considered, which make the problem more complicated [44].
- Mostly multi-objective algorithms based on the GA, PSO, ACO, and ABC are used for MPOPs, but many-objective algorithms such as NSGA-III, MOEA/D are rarely found in literature [43]. Even in the literature of generalized optimization, data-driven NSGA-III is not yet available.
- While discussing the surrogate-assisted optimization, comparative analyses based on the different surrogate models are performed rarely [40].
- Most of the research works are based on the empirical real-world data; however, the systematic MPOP test data or published data are not yet available in cumulative forms for the algorithmic testing. Eleven test data are identified and grouped with the Best Solutions Found (BSF) and made available in the online data repository [45].

Therefore, an aim is made in this research to develop a data-driven NSGA-III for multi-response MPOPs. The proposed approach exploits a deep-learning based surrogate model as the objective function. For that matter, three different deep-learning models based on MLP/Feed Forward ANN, GKR, and GRNN are employed and the best performing surrogate is picked. The proposed data-driven approach is verified with the MPOP test data from the repository and promising results are obtained.

3. Data-Driven NSGA-III

In order to develop the proposed technique, three different deep-learning based approaches are studied, feed forward neural network (FFNN), GKR, and GRNN. These tools are substantially efficient in producing suitable approximation models for the machining processes.

3.1. FFNN

FFNN is an apt tool for surrogate modeling because it is naturally proficient in approximating outputs from the arbitrary input parameters [38]. The FFNN diagram is portrayed in Figure 3. It has n input neurons, m hidden layers neurons, and two output neurons. The output equation of the FFNN is stated as,

$$y_i = Z_i^{oa}\left(\sum_{j=1}^{m} w_{ji}^{oa} \times Z_k^{ha}\left(\sum_{k=1}^{n} w_{jk}^{ha} x_k\right)\right) \quad (1)$$

Where Z_i^{oa} is the activation function for i^{th} output y_i, w_{ji}^{oa} is the weight from j^{th} hidden layer node to i^{th} output node, Z_k^{ha} is the activation function for j^{th} hidden layer neuron, w_{jk}^{ha} is the weight from k^{th} input to j^{th} hidden layer neuron, and x_k is k^{th} input signal. Further, if some bias is added to input layer, the equation (1) becomes,

$$y_i = Z_i^{oa}\left(\beta_i + \sum_{j=1}^{m} w_{ji}^{oa} \times Z_k^{ha}\left(\beta_j + \sum_{k=1}^{n} w_{jk}^{ha} x_k\right)\right) \quad (2)$$

Where β_i is the weight from the bias to the i^{th} output node and β_j is the weight from the bias to j^{th} hidden layer neuron.

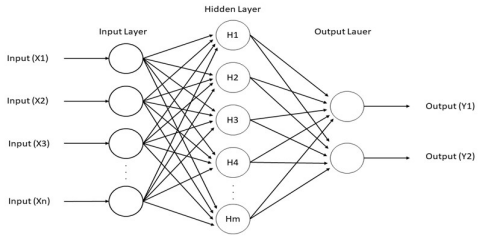

Figure 3. FFNN diagram

3.2. GRNN

GRNN estimates the responses using weighted average of the outputs of the training data. The weights are computed using the euclidean distance between the training and testing data, which are also termed as activation functions. Weights and computed distances are inversely proportional. GRNN contains the input layer, hidden layer, summation layer, and output layer nodes (Figure 4). Input layer takes the input data and pass on to the next layers, where the euclidean distances and activation functions are computed. In summation layer, two sub-components are integrated namely, the numerator (N) and denominator (D), which perform summation of the multiplication of the

training data and activation function and summation of all the activation functions respectively. Finally, in output layer, one neuron is portrayed, which computes the overall response using the ratio of N and D from summation layer [46]. The response equation of GRNN is,

$$y = \frac{\sum_i y_i \, e^{-\left(\frac{d_i^2}{2\sigma^2}\right)}}{\sum_i e^{-\left(\frac{d_i^2}{2\sigma^2}\right)}} \tag{3}$$

Where $d_i^2 = (x - x_i)^T(x - x_i)$ is the euclidean distance between x and x_i, $e^{-((d_i\hat{}2)/(2\sigma\hat{}2))}$ is the activation function and σ is the spread constant, which could be adjusted to hold the optimal value using GRNN training so that the mean square error (MSE) value converges to zero.

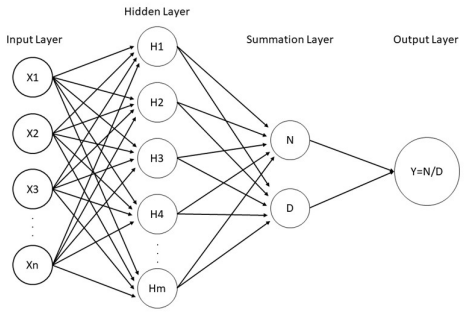

Figure 4. GRNN Diagram

3.3. GKR

GKR is based on the data mapping from the low dimensional space to high dimensional space. Since it is a linear regression model in high dimensional space, therefore, it is equivalent to the Gaussian regression in low dimensional space. The linear regression learner used, is based on the SVM regression. In this approach, the input parameters x are mapped onto an m-dimensional attribute space using specific nonlinear mapping, which further converts it to a linear model in the same attribute space. The linear model is expressed as,

$$f(x, \omega) = \sum_{j=1}^{m} \omega_j g_j(x) + \beta \tag{4}$$

Where $g_j(x)$ $(j=1\ldots m)$ is a non-linear transformation function and β is the bias. The performance of regression is analyzed using the ε-insensitive loss function [47],

$$L\big(y, f(x,\omega)\big) = \begin{cases} 0 & if\ |y - f(x,\omega)| \le \varepsilon \\ |y - f(x,\omega)| - \varepsilon & Otherwise \end{cases} \tag{5}$$

The observed risk is,

$$R(\omega) = \frac{1}{n}\sum_{i=1}^{n} L(y_i, d(x_i, \omega)) \tag{6}$$

The abovementioned regression model can be transformed into an optimization problem using,

$$\min Z = \frac{1}{2}\|\omega^2\| + C\sum_{k=1}^{n}(\gamma_i + \gamma_i^*) \tag{7}$$

Subject to,

$$\begin{cases} y_i - f(x_i, \omega) \le \varepsilon + \gamma_i^* \\ f(x_i, \omega) - y_i \le \varepsilon + \gamma_i \\ \gamma_i, \gamma_i^* \ge 0, i = 1 \ldots n \end{cases} \tag{8}$$

Where γ_i and γ_i^* $(i=1\ldots n)$ are the positive slack variables, which can calculate the deviation of the input parameters beyond the ε-insensitive neighborhood. This optimization problem is known as *primal*. In exact SVM regression, this could be transformed into a *dual* and solved using an exact SVM kernel, whereas, in SVM assisted GKR model, the *primal* is solved using the high-dimensional attribute space. Therefore, the kernel function is approximated thereon [48].

3.4. Performance Metric

In this study, MSE is used as the performance measure for the abovementioned surrogate models. MSE is a metric that measures the overall deviations between the predicted and measured values. It is defined as,

$$MSE = \frac{1}{N}\sum_{i=1}^{N}(Y_i - T_i)^2 \tag{9}$$

Where Y is the approximated output, T is the target output, and N is the number of observations. The lower MSE score indicates the higher accuracy in space and time [49]. The most optimal surrogate model is selected based on the lowest MSE score obtained in this study.

3.5. NSGA-III

NSGA-III is a state-of-the-art many-objective optimization technique proposed by Deb and Jain [44]. NSGA-III is developed on the framework of its predecessor NSGA-II with a modified selection strategy. NSGA III is based on a uniformly generated set of reference points in the objective space, which are updated using supervised learning. The algorithm is described in algorithm 1. NSGA-III begins with some initial population POP of size N using random function, and predefined set of reference points Z^{ref}. The algorithm executes for a prefixed number of iterations. While in execution, the tournament selection, binary crossover, and polynomial mutation [50] operators are applied on the POP, it generates exactly same number of offspring solutions (new child population is POP_{new}).

Algorithm 1: NSGA III

1: **Generate** the reference points Z^{ref} to be placed on the hyper plane
2: **Generate** initial population *POP* at random
3: **Generate** Ideal points Z^{max}
4: **Evaluate** *POP* using Fitness Function and **perform** the non-dominated sorting on POP
5: **for** i=1 to Maximum number of generation (*maxGEN*) **do**
7: **Perform** the crossover on POP (probability: P_c)
8: **Perform** the mutation on POP (probability: P_m)
9: **Add** new solutions to POP_{new} and obtain POP= POP ∪ POP_{new}
8: **Perform** the non-dominated sorting on POP
9: **Normalize** the POP using Z^{max}
10: **Associate** the population member with the Z^{ref}
11: **Calculate** the number of niche and **perform** the niche preservation
12: Obtain and pass the niche obtained population members to the next generation
13: **end for**

Further the new population is formed as, $POP = POP \cup POP_{new}$ (size $2N$). Then the non-dominated sorting technique is applied based on domination mechanism [51]. This procedure could group the members in new population *POP* using different ranking system ($F_{i \text{ where } i=1,2,\ldots,n}$). The population for the next iteration is then obtained based on this ranking system. For an example, F_1 members would be included first, then F_2 and so on. This way, the population of size N is chosen. If the l^{th} rank members are the last to be included in next population. Then, $(l+1)^{th}$ onwards all the members are rejected. At this point, not all the members with F_l rank might be considered due to the space constraint (population size N). Hence, reference point based selection mechanism is employed, which differs from the crowding distance based method of NSGA-II [52]. The said method is demonstrated next.

The *reference points* are obtained using the procedure defined by [53], which arranges the reference points on the normalized hyper-plane. Pareto solutions are normally associated with the reference points on the hyper-plane. This hyper-plane is inclined to the M-objective axes and defined using an $(M-1)$-dimensional unit simplex. The number of the reference points are decided on the number of divisions of each of the objective axes. For P number of divisions, the number of reference points H would be computed as,

$$H = C_P^{M+P-1} \tag{10}$$

The *normalization* procedure proposed by Deb and Jain [44] helps identify the set of ideal points Z^{max} by solving a set of linear equations, which is computationally expensive. To make it simple, the simplified normalization procedure is followed. If $Z_j^{min} = (z_1^{min}, z_2^{min}, \ldots, z_M^{min})$ is the set of ideal points with the minimum objective values for j^{th} member $\forall\ j \in [1, N]$. z_l^{min} is the l^{th} lowest objective value $f_i\ \forall\ i \in [1, M]$. The $z_l^{max} \in Z^{max}$

is supposed as the worst point for the i^{th} objective. The normalized objective value $fi^*(x_j)$ is calculated using Eq. (11).

$$f_i^*(x_j) = \frac{z_i^{max} - f_i(x_j)}{z_i^{max} - z_i^{min}} \quad \forall i \in [1, M] \; and \; \forall j \in [1, N] \qquad (11)$$

Once the objective values are normalized, each population member is mapped to a reference point. For that matter, the reference lines are drawn from each of the reference points to the origin in the hyper-plane. Then, the perpendicular distance between each population member and each reference line is computed. For every reference point, the minimum perpendicular distance is calculated, and the corresponding population member is mapped to that reference point.

Niches are matched for each reference point based on the associated population member. Niche preservation is performed to select the desired candidates from F_l (the last selected level from new POP) using the following rule. First, the reference points set is selected with minimum niche counts. If the number of such reference points are more than one, a random reference point is selected from above set. If the niche count is zero, the member is chosen based on the smallest perpendicular distance to the reference line else if the niche count is one or greater, a random member is selected from F_l front. Thereafter, the niche count is increased by one for the next iteration of the niche preservation procedure. If this selection operation is exhausted for a reference point, then that is excluded from the present iteration. This niche preservation procedure is repeated for the $N - |POP|$ times (until the new population is filled). Finally, the new population of size N is obtained. The proposed data-driven surrogate-assisted NSGA-III framework is portrayed in Figure 5.

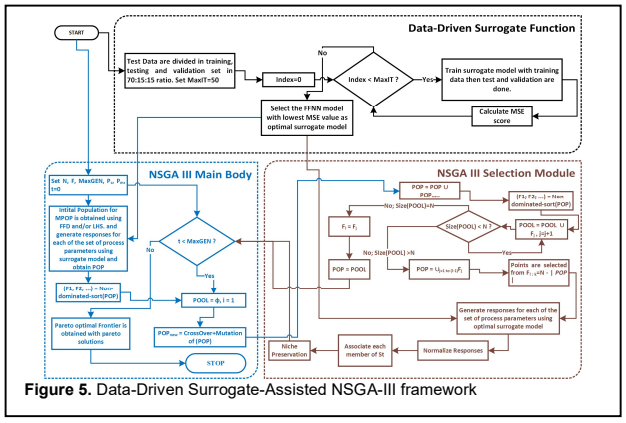

Figure 5. Data-Driven Surrogate-Assisted NSGA-III framework

4. Results and Discussions

In this research, eleven real-world cases are collected based on machining processes from the related literature. These are based on the turning, grinding, heat exchanger tube, milling, abrasive water jet machining, dry turning, drilling, welding, and emulsification processes. These cases are used as test data for the proposed data-driven NSGA III algorithm. These data are readily available from the online repository for further research with BSF values [45]. Details of the data are presented in Table 1. The last column of Table 1 depicts the type of objectives considered for each data. If the response is Higher-the-Better, it is denoted as 'Max', if it is Lower-the-Better, it is denoted as 'Min' and 'Nominal-the-Better', it is denoted as 'Nom'. The proposed data-driven NSGA-III algorithm is implemented in MATLAB R2018a on Intel 8650U @1.90GHz computer. For the purpose of comparison, another well-versed many-objective algorithm, MOEA/D [54] is considered in this study. The difficulty of the data-driven surrogate-assisted optimization algorithms could amplify insanely with the number of process parameters and performance characteristics for the MPOPs. These data are divided in 70:30 for the training, and testing. Table 2 portrays a comparative analysis of the training of surrogate models considered, which are FFNN, GKR, and GRNN. Comparison is performed based on the obtained MSE values and it reveals that the GKR surrogate is more accurate than other two. Therefore, based on the MSE scores, the GKR is selected for further study.

Table 1. Details of eleven cases collected from literature

No.	Ref.	Data Size	No. of variables	No. of Responses	Type of Responses*
1	55	9×8	5	3	m m m
2	56	9×7	4	3	m m m
3	57	18×7	4	3	M m M
4	58	27×8	5	3	m m m
5	59	9×7	3	4	m m m m
6	60	18×8	4	4	m m m M
7	61	16×9	5	4	m m M m
8	62	9×7	3	4	M N N m
9	63	27×8	3	5	m m m m m
10	64	18×12	4	8	All M
11	65	18×12	4	8	M M m M M m m m

M: Higher-the-Better (Maximization); m: Lower-the-Better (Minimization); N: Nominal-the-Better (Any)

Table 2. Comparison results of the surrogate models based on MSE

MSE	GKR	FFNN	GRNN
Data #1	**1.07142**	2.5863	1.32591
Data #2	**0.04915**	1.2327	0.65281
Data #3	**61.74**	1432.60	528.0789
Data #4	**3076.308**	6674.50	37210.00
Data #5	**1.95**	41.4584	68.0058
Data #6	**670.2691**	872.2372	1053.50
Data #7	**217.0276**	475.5653	2029.60
Data #8	**24.82035**	1263.80	302.0497
Data #9	**63.5038**	804.1896	76.2148713
Data #10	**185.8598**	378.1857	387.6465
Data #11	**185.8598**	378.1857	387.6465

For both the algorithms, NSGA-III and MOEA/D, identical set of parameters are considered for all the test cases. Probability of crossover is set to 0.5 and mutation rate is set to 0.02. These parameters are set after at least 50 independent runs. Population size, number of generations and initial population generation techniques differ depending on the size of the data and number of the objectives. The details are presented in Table 3. For the purpose of this study, different initial solution generation procedures are adopted here. For the surrogate-assisted optimization techniques, popular DOE tools are practiced mostly with an aim to obtain an evenly distributed problem design space, which is logically random. FFD is a popular DOE tool, which has rarely been practiced for the population generation in surrogate-assisted optimization. The possible reason would be the limited number of experimental runs are defined for the FFD. For an example, data #5 has three parameters with three levels, hence the FFD based design space is set to 3^3 (=27). The proposed NSGA-III based technique is initialized with a population size of 200. Therefore, remaining 173 combinations of design parameters are generated using another popular DOE tool called LHS [65]. This way, the diversity in design space is maintained. The last column of Table 3 depicts the types of DOE techniques used and the number of generated solutions by these tools respectively.

Table 3. Parameters and choice of DOE tools for the algorithms for various data

	Population Size	Number of Iteration	Initial Population Generation Technique
Data #1	81	50	FFD (3^4=81)
Data #2	81	50	FFD (3^4=81)
Data #3	81	50	FFD (3^4=81)
Data #4	243	50	FFD (3^5=243)
Data #5	200	50	FFD (3^3=27) + LHS (173)
Data #6	200	50	LHS (200)
Data #7	200	50	LHS (200)
Data #8	200	50	FFD (3^3=27) + LHS (173)
Data #9	200	50	FFD (3^3=27) + LHS (173)
Data #10	200	50	FFD (3^4=81) + LHS (119)
Data #11	200	50	FFD (3^4=81) + LHS (119)

First four data represent three-objective MPOPs. Table 4 and Table 5 portray the holistic results obtained for these problems using the NSGA III and MOEA/D. The published results and the most promising

Pareto solutions obtained using the MOEA/D and NSGA-III are presented in Table 4.

Table 4. Results obtained using MOEA/D and NSGA-III for three-objective MPOPs

#	Published Results	MOEA/D Results	NSGA-III Results
Data #1	CS=155.000, FR=0.120, CD=0.800, CFR=12.000, Ra=1.028, Rt=4.530, Phi=0.740	(1) CS=181.203, FR=0.120, CD=0.737, CFR=11.974, Ra=0.367, Rt=2.949, Phi=0.142	(1) CS=131.624, FR=0.120, CD=0.730, CFR=6.034, Ra=0.569, Rt=2.136, Phi=0.135
Data #2	DF=5, GF=6, DT=2.5, CT=11, Ra=0.439, OC=0.667, DT=-0.001	(1) DF=7.827, GF=9.784, DT=2.406, CT=10.590, Ra=0.325, OC=0.053, DT=0.001	(1) DF=4.996, GF=8.106, DT=2.851, CT=11.866, Ra=0.355, OC=0.134, DT=0.002
Data #3	Re=23000, PR=3,DR=0.7, PI=24, Nu=134.22, f=0.14, n=1.23	(1) Re=23000, PR=3, DR=0.8, PI=24, Nu=135.2004, f=0.0805, n=1.3094	(1) Re=6500, PR=1, DR=0.729, PI=23.84, Nu=131.83, f=0.0096, n=1.375
Data #4	WP=320, AMF=200, TS=8, SOD=5, MT=18, TKW=1050.5, IRA=3.01, ZRA=3.54	WP=279.2696, AMF=248.997, TS=7.631, SOD=5.266, MT=20.0396, TKW=1312.552, IRA=2.49, ZRA=3.455	WP=290.276, AMF=260.098, TS=7.166, SOD=5.42, MT=18.174, TKW=1270.65, IRA=0.126, ZRA=2.57

The boundary conditions are provided as 125 ≤ CS ≤ 185, 0.12 ≤ FR ≤ 0.2, 0.5 ≤ CD ≤ 0.8, and 4 ≤ CFR ≤ 12 for data #1. For data #2, these are 5 ≤ DF ≤ 10, 2 ≤ GF ≤ 10, 1.5 ≤ DT ≤ 3, 10 ≤ CT ≤ 12. For data #3, these are 6500 ≤ Re ≤ 23000, 1 ≤ PR ≤ 3, 0.6 ≤ DR ≤ 0.8, 8 ≤ PI ≤ 24. For data #4, these are 260 ≤ WP ≤ 320, 200 ≤ AMF ≤ 350, 2.5 ≤ TS ≤ 8, 5 ≤ SOD ≤ 10, 18 ≤ MT ≤ 38. The results obtained by NSGA III satisfy the abovementioned boundary conditions and the results of MOEA/D are within the boundary. It could be observed that the results obtained for data #1 and #3 are better than the published results for all objectives, whereas, obtained results are better for at least two objectives for data #2 and #4. NSGA-III results are competitive with MOEA/D results. Table 5 shows the statistical details of the obtained Pareto frontiers of the NSGA-III and MOEA/D. It could be inspected that the obtained solutions do not deviate much from the best results; therefore, the mean objective values are better than published values. This implies that, both the techniques are equally good and capable of obtaining optimal solutions. NSGA-III is better for some of the objectives and MOEA/D is better for other objectives. Similar analyses could be presented for data #5 to data #8. These are four-objective MPOPs. The overall results are portrayed in Table 6 and Table 7. Table 6 demonstrates that at least one Pareto solution for each of the algorithms would be competitive with the published results.

Table 5. Statistical details of Pareto solutions for three-objective MPOPs

		MOEA/D				NSGA-III			
		Data 1	Data 2	Data 3	Data 4	Data 1	Data 2	Data 3	Data 4
Obj 1	Min	0.24569	0.16983	27.412	1214.154	0.44846	0.35545	11.0018	1050.5
	Max	1.9681	0.439	161.4545	1312.552	1.1522	0.40725	185.7585	1395.79
	St. Dev	0.18126	0.10209	41.9602	16.7464	0.25508	0.011602	27.0774	88.1401
	Mean	**0.37792**	**0.3587**	110.287	1239.815	0.85867	**0.38542**	**166.2197**	**1086.56**
Obj 2	Min	1.5725	0.009723	0.00033	2.4915	0.28585	0.13366	0.00694	0.026106
	Max	12.652	1.9179	1.2712	6.3796	12.9064	0.74991	0.24851	3.5819
	St. Dev	1.3136	0.30932	0.32137	0.54317	3.7717	0.14837	0.043699	0.95718
	Mean	3.5379	0.62582	0.4255	5.2895	**2.8578**	**0.48444**	**0.15274**	**2.6196**
Obj 3	Min	0.000111	-.001	0.82621	0.29885	0.000642	0.001092	1.0249	0.000379
	Max	0.89778	0.009165	1.3551	3.4548	0.88406	0.002204	1.3783	20.0964
	St. Dev	0.13957	0.002006	0.13429	0.44493	0.18841	0.000247	0.057411	1.7875
	Mean	**0.1171**	**0.000163**	1.05	**1.3147**	0.29548	0.001506	**1.0662**	3.5201

Table 6. Results obtained using MOEA/D and NSGA-III for four-objective MPOPs

#.	Published Results	MOEA/D Results	NSGA-III Results
Data #5	SS=10000, FPT=0.5, DC=50, TW=5.41, Fx=1.33, Fy=0.71, Ra=0.33	SS=10106.1766, FPT=0.621, DC=51.266, TW=3.932, Fx=1.3096, Fy=0.70787, Ra=0.3235	SS=10097.956, FPT=0.5563, DC=50.00687, TW=0.668, Fx=1.3016, Fy=0.7656, Ra=0.31845
Data #6	NR=0.4, CS=78.9, FR=0.05, DC=0.4, Fx=49.03, Fy=31.06, Fz=148.74, MRR=0.355	NR=0.4, CS=84.0844, FR=0.05, DC=0.469, Fx=50.739, Fy=39.726, Fz=124.5196, MRR=0.443	NR=0.591, CS=93.763, FR=0.136, DC=0.4766, Fx=73.054, Fy=31.946, Fz=201.198, MRR=0.5825
Data #7	SC=40, PTEM=900, PTIM=7.5, SINTEM=1175, SINTIM=15, PD=0.89, WA=3, BR=178.9, LOI=5.4	SC=29.89, PTEM=583.01, PTIM=9.12, SINTEM=1192.39, SINTIM=17.105, PD=0.213, WA=0.033, BR=244.0135, LOI=2.2	SC=21.62, PTEM=537.126, PTIM=20.523, SINTEM=1177.45, SINTIM=23.43, PD=0.569, WA=7.553, BR=185.41, LOI=6.38
Data #8	SC=1, SS=5000, WC=5, SP=284, HV=42.6, DEN=839.6, KV=2.6	SC=1.165, SS=11201.648, WC=9.032, SP=319.036, HV=42.058, DEN=844.861, KV=3.390	SC=1.135, SS=13188.997, WC=13.019, SP=272.335, HV=41.308, DEN=844.783, KV=2.826

The boundary conditions for data #5 are defined as 10000 ≤ SS ≤ 12000, 0.5 ≤ FPT ≤ 1.5, 50 ≤ DC ≤ 100. For data #6, these are 0.4 ≤ NR ≤ 0.8, 46.65 ≤ CS ≤ 102.63, 0.05 ≤ FR ≤ 0.2, 0.4 ≤ DC ≤ 0.8. For data #7, these are 10 ≤ SC ≤ 40, 300 ≤ PTEM ≤ 900, 7.5 ≤ PTIM ≤ 30, 1125 ≤ SINTEM ≤ 1750, 10 ≤ SINTIM ≤ 25. For data #8, these are 0.5 ≤ SC ≤ 1.5, 5000 ≤ SS ≤ 15000, 5 ≤ WC ≤ 15. All the obtained results satisfy the abovementioned boundary conditions.

Table 7. Statistical details of Pareto solutions for four-objective MPOPs

		MOEA/D				NSGA-III			
		Data 5	Data 6	Data 7	Data 8	Data 5	Data 6	Data 7	Data 8
Obj 1	Min	0.022237	23.0473	0.006133	146.0032	0.66785	66.0081	0.19874	229.3933
	Max	27.9096	180.1501	1.6406	338.022	7.1214	140.8389	0.68134	272.3345
	STD	4.876	31.6443	0.22175	51.7184	0.83605	14.5289	0.082832	7.401
	Mean	4.252	**71.911**	**0.15145**	**260.5149**	**3.7788**	95.5652	0.38498	254.8826
Obj 2	Min	1.1067	30.1429	0.001057	38.5953	1.3016	28.7855	6.0464	40.8999
	Max	2.5852	122.4458	5.1703	44.4466	1.4433	65.8542	12.9593	41.3348
	STD	0.29808	26.5538	0.65348	1.2645	0.018055	6.8823	1.117	0.063375
	Mean	1.51	68.6461	**0.44268**	**41.9475**	**1.3732**	**41.627**	8.3496	41.1674
Obj 3	Min	0.62691	101.4875	175.9111	827.4191	0.71001	184.4619	140.7625	844.7681
	Max	1.2445	383.2257	271.2379	868.0094	0.76559	302.068	199.1408	850.1016
	STD	0.12176	67.9347	17.0271	7.4934	0.009242	23.0157	9.4422	0.90535
	Mean	0.7871	**219.4054**	**230.4393**	844.9152	**0.73894**	231.1358	165.5958	**846.7218**
Obj 4	Min	0.12111	0.33027	0.83344	1.3745	0.30294	0.46416	6.0626	2.3731
	Max	0.48036	1.7384	4.5454	5.8653	0.36287	1.3621	7.5945	3.0689
	STD	0.087133	0.28772	0.54979	0.98102	0.010076	0.18255	0.26897	0.11872
	Mean	**0.28721**	0.72804	**1.7887**	3.1798	0.32783	**0.85929**	6.9433	**2.7091**

For data #5, the objective scores obtained by NSGA-III and MOEA/D outperforms the published results. For data #6, at least two objective scores are better than the published results. More important objective is MRR than the cutting forces [60], which shows improved values for both the algorithms. For data #7, MOEA/D shows better results than the NSGA-III by producing best scores, whereas NSGA-III obtains good scores for at least two objectives. In case of data #8, NSGA-III obtains very close values to the published results. Table 7 depicts statistical details of obtained results for data #5-#8. The Mean values obtained by the MOEA/D and NSGA-III are good are improved. This further proves

that the obtained Pareto frontiers are near optimal and convergence properties are tight to the solution spaces.

Table 8. Results obtained using MOEA/D and NSGA-III for five to eight objective MPOPs

Data No.	Published Results	MOEA/D Results	NSGA-III Results
Data #9	SS=3000, PA=100, FR=100, TF=84.23, TOR=0.39, EnDF=1.4287, ExDF=1.41, Ecc=0.0156	SS=1915.342, PA=102.117, FR=155.611, TF=81.079, TOR=0.193, EnDF=1.436, ExDF=1.405, Ecc=0.010	SS=1472.946, PA=109.898, FR=161.275, TF=73.769, TOR=0.826, EnDF=1.366, ExDF=1.339, Ecc=0.011
Data #10	PD=0.12, TRS=1100, WS=98, SD=24, UTS=135.05, YS=113.25, E=5.37, CS=8.02, BA=45, AHNZ=55.26, AHTMAZ=53.09, AHHAZ=49.12	PD=0.204, TRS=971.365, WS=98.717, SD=23.627, UTS=131.857, YS=103.503, E=6.978, CS=5.812, BA=53.189, AHNZ=56.783, AHTMAZ=62.183, AHHAZ=52.187	PD=0.181, TRS=769.885, WS=82.647, SD=22.194, UTS=79.786, YS=70.254, E=4.236, CS=8.394, BA=45.568, AHNZ=57.138, AHTMAZ=57.910, AHHAZ=51.568
Data #11	PD=0.21, TRS=600, WS=98, SD=24, UTS=113.04, YS=109.64, E=1.46, CS=5.23, BA=35, AHNZ=52, AHTMAZ=50.36, AHHAZ=48.66	PD=0.170, TRS=600, WS=98, SD=24, UTS=132.174, YS=111.654, E=1.413, CS=6.879, BA=39.206, AHNZ=53.820, AHTMAZ=51.945, AHHAZ=50.742	PD=0.148, TRS=728.862, WS=87.578, SD=19.21, UTS=131.221, YS=119.673, E=0.589, CS=5.125, BA=44.636, AHNZ=51.517, AHTMAZ=49.029, AHHAZ=49.738

For the rest of the data (#9-#11), the number of objectives is higher. The results are portrayed in Table 8. The boundary conditions are defined as $1000 \leq SS \leq 3000$, $100 \leq PA \leq 135$, $100 \leq FR \leq 500$ for data #9. For data #10 and #11, these are $0.12 \leq PD \leq 0.21$, $600 \leq TRS \leq 1100$, $63 \leq WS \leq 132$, $16 \leq SD \leq 24$. Both the EAs satisfy the

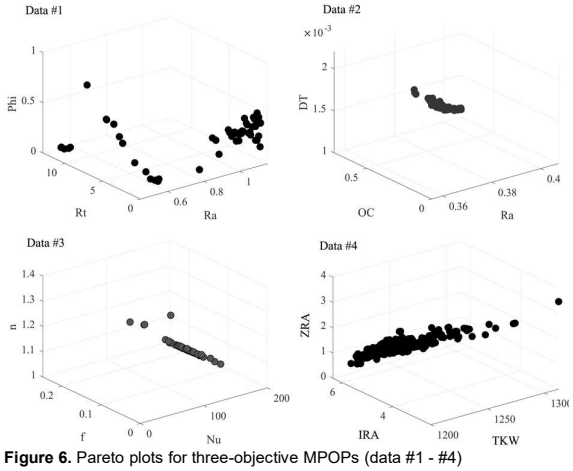

Figure 6. Pareto plots for three-objective MPOPs (data #1 - #4)

abovementioned boundary conditions. For data #9, it is observed that the objective values are better for at least four out of five responses. The NSGA-III obtains slightly better results than the MOEA/D. Rest of the cases are identical except the types of the responses considered. Table 9 and Table 10 portray statistical details for the Pareto solutions obtained for these data.

Table 9. Statistical details of Pareto solutions for data #9

		MOEA/D	NSGA-III
Obj1	Min	89.9676	67.4746
	Max	316.8432	203.0775
	STD	46.9734	47.4164
	Mean	171.7997	**169.6964**
Obj2	Min	0.4363	0.19287
	Max	1.8016	1.6763
	STD	0.28929	0.45359
	Mean	**0.83595**	1.3899
Obj3	Min	1.1919	1.3295
	Max	1.5758	1.4355
	STD	0.076778	0.02088
	Mean	**1.3661**	1.3852
Obj4	Min	1.1797	1.232
	Max	1.5034	1.4522
	STD	0.074801	0.058484
	Mean	1.3492	**1.2846**
Obj5	Min	0.013958	0.000236
	Max	0.094262	0.062879
	STD	0.013388	0.014728
	Mean	0.048773	**0.019597**

Table 10. Statistical details of Pareto solutions for data #10 and data #11

		MOEA/D		NSGA-III	
		Data 10	Data 11	Data 10	Data 11
Min	Obj1	66.193	108.54	64.10	65.094
Max		143.2	152.76	86.13	140.26
STD		13.583	9.5639	3.245	16.369
Mean		**120.38**	**130.94**	79.79	111.29
Min	Obj2	63.378	85.326	61.57	52.000
Max		164.36	113.23	81.60	131.08
STD		22.572	6.1076	2.802	16.128
Mean		**97.212**	97.933	70.39	**103.59**
Min	Obj3	2.365	1.0386	3.291	0.0300
Max		10.415	2.0119	5.170	5.7989
STD		2.128	0.1739	0.271	1.1034
Mean		**5.985**	1.6994	4.269	**1.423**
Min	Obj4	0.945	1.5257	6.799	2.75
Max		10.66	7.1936	10.34	7.9823
STD		2.067	0.7325	0.656	0.9148
Mean		6.957	**5.411**	**8.719**	5.1429
Min	Obj5	14.36	15.43	27.588	10.893
Max		76.71	43.91	59.274	75.423
STD		10.16	4.074	5.1583	12.097
Mean		**47.58**	34.27	44.160	**42.574**
Min	Obj6	46.09	52	55.242	46.201
Max		61.65	62.1	59.495	59.948
STD		3.942	0.917	0.7323	2.3591
Mean		55.83	58.81	**57.531**	**51.251**
Min	Obj7	50.82	50.36	52.672	48.383
Max		62.83	53.67	62.000	60.815
STD		3.656	0.301	1.5957	2.051
Mean		**58.69**	53.18	57.735	**50.071**
Min	Obj8	48.96	48.66	50.015	45.984
Max		53.87	51.53	52.226	50.377
STD		1.338	0.284	0.3134	0.6951
Mean		**51.66**	50.69	51.383	**49.242**

Table 11. CPU time (Seconds) consumed by both the EAs

	Data 1	Data 2	Data 3	Data 4	Data 5	Data 6
MOEA/D	33.552	32.019	34.847	139.21	114.226	115.834
	Data 7	Data 8	Data 9	Data 10	Data 11	
	116.66	117.574	169.292	2304.23	1764.77	
NSGA-III	Data 1	Data 2	Data 3	Data 4	Data 5	Data 6
	34.452	32.527	29.238	113.352	86.3906	86.9707
	Data 7	Data 8	Data 9	Data 10	Data 11	
	82.806	88.9076	95.2284	1225.181	1224.518	

Obtained solutions are evenly distributed in the solution space. Therefore, the obtained solutions portray improved mean and standard deviation scores. This is also depicted that the individual objective scores are optimal and objective tradeoffs are obtained accordingly.

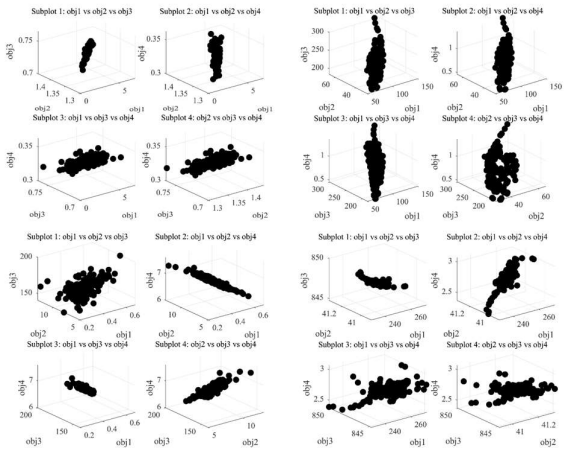

Figure 7. Pareto plots for four-objective MPOPs (data #5 - #8)

Table 11 portrays the CPU times consumed by both the EAs and the NSGA-III works faster that MOEA/D. Objective trade-offs for data #1 to #9 are portrayed in Fig. 6-8. These are 3-5 objective problems. Another example of the largest data #10 (eight objectives) is portrayed using the parallel coordinate plots in Fig. 9.

For the machining related process optimization, the validation or confirmatory tests are required. Otherwise, the results obtained by data-driven optimization algorithms do not provide any relevant information. Since the test data are considered from the literature and due to the involvement of various types of the machining operations, it is not possible to verify the obtained results. However, the rigorous tests on enough test data would confirm the consistency of the proposed techniques. The conformity of the obtained results within the boundary conditions for the MPOPs proves the relevancy of the performances of algorithms. Further, a statistical test is conducted to validate the results obtained by the data-driven EAs.

4.1. Statistical Analysis

The objective of this statistical test is to measure the performances of the EAs in the state space. For that matter, the euclidean distance between multi-objective solutions (BFS and EA solutions) are computed using,

$$dist(z_1, z_2) = \sqrt{\sum_{i=1}^{m} \left(f_i(z_1) - f_i(z_2)\right)^2} \quad (12)$$

Where z_1 and z_2 are the solutions and $f_i(z_1)$ and $f_i(z_2)$ are the fitness values for i^{th} objective. In this analysis, the solution diversity is considered as the measurement. Therefore, the Front Spread (FS) indicator is incorporated [66]. The FS metric measures the objective space area covered by the solution set POP. The larger is the obtained FS value; the better is the performance of the corresponding EA. For m-dimensional state space consisting of POP, the FS is computed using,

$$FS(POP) = \sqrt{\sum_{i=1}^{m} max_{(z_1,z_2)\in POP\times POP} \left\{\left(f_i(z_1) - f_i(z_2)\right)^2\right\}} \quad (13)$$

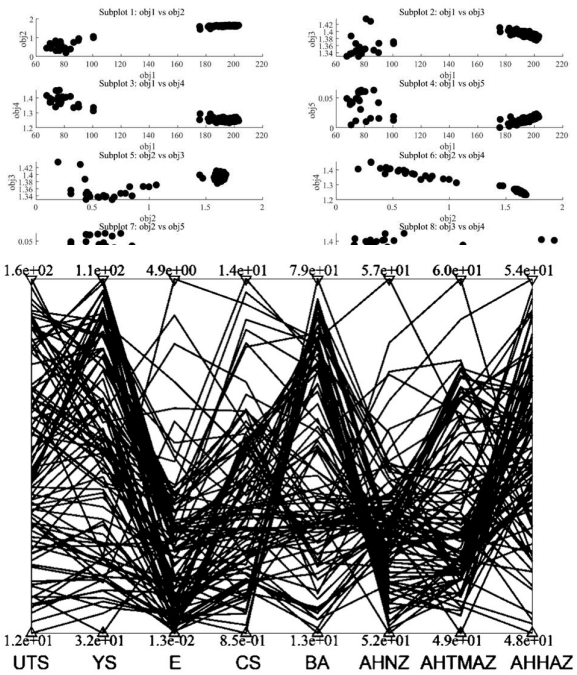

Figure 9. Pareto plot for eight-objective MPOP (data #10) (Responses are ultimate tensile strength (UTS), yield strength (YS), percentage of elongation (% E), compressive stress (CS), bending angle (BA), average hardness at the nugget zone (AHNZ), thermo mechanical affected zone (AHTMAZ) and heat affected zone (AHHAZ))

To facilitate the statistical analysis, the numerical FS scores are computed for all the results (Table 12). These FS scores are considered as two independent sets of values. Therefore, the equality of variances is tested with 2 variances f-test with σ_1: standard deviation of MOEA/D; σ_2: standard deviation of NSGA III. The ratio σ_1/σ_2 is the indicator. If the test statistic < critical value ($F < F_{critical}$) accept the null hypothesis; in other words, if *p*-value > α, accept the null hypothesis. The f-test result is shown in Table 13. According to the result, it is clearly visible that the F < Fcritical (2.671217985 < 2.978237016); p-values > α (0.068499784>0.05). Therefore, the null hypothesis is accepted, and it is concluded that the variances are equal. Further, the paired t-test is performed assuming equal variances. The result of t-test is reported in Table 14. If the test statistic < critical value (F < Fcritical) accept the null hypothesis; in other words, if p-value > α, accept the null hypothesis. Since the null hypothesis is that the mean difference = 0, therefore this would be decided with a two-sided test. Two-tail values are used for the analysis. According to Table 14, the test statistic < critical values (0.776115333 < 1.812461123 and 0.776115333 < 2.228138852) and the p-values for one-tail and two-tail > α (0.227822418 > 0.05 and 0.455644837 > 0.05), thus the null hypothesis is accepted, and the means are same. Therefore, the obtained results are consistent and reliable. More specifically, it could also be stated that, even though the NSGA III (mean= 34.2572) performs little better than the MOEA/D (mean= 46.1848), they are equally capable of producing reliable solutions for the MPOPs.

Table 12. FS scores by both the EAs

Data #	MOEA/D	NSGA III
1	1.340E+00	1.738E+00
2	8.990E-02	1.908E-01
3	2.394E+01	3.200E+01
4	1.893E+02	3.606E+01
5	1.175E+00	1.632E+00
6	8.325E+01	9.522E+01
7	5.173E+01	1.443E+01
8	2.410E+01	3.001E+01
9	8.757E+01	8.547E+01
10	2.278E+01	7.018E+01
11	2.273E+01	9.897E+00

Table 13. F-Test Two-Sample for Variances

	MOEA/D	*NSGA III*
Mean	46.18487273	34.25720909
Variance	3185.430948	1192.501311
Observations	11	11
df	10	10
F	2.671217985	
P(F<=f) one-tail	0.068499784	
F Critical one-tail	2.978237016	

Table 14. t-Test: Paired Two Sample for Means

	MOEA/D	*NSGA III*
Mean	46.18487273	34.25720909
Variance	3185.430948	1192.501311
Observations	11	11
Pearson Correlation	0.4566072	
Hypothesized Mean Difference	0	
df	10	
t Stat	0.776115333	
P(T<=t) one-tail	0.227822418	
t Critical one-tail	1.812461123	
P(T<=t) two-tail	0.455644837	
t Critical two-tail	2.228138852	

5. Conclusions

An attempt has been made in this article to implement the data-driven surrogate-assisted EAs to optimize the manufacturing processes. These types of optimization problems are based on the limited off-line data. The proposed technique is based on the NSGA-III algorithms. The proposed data-driven technique exploited the GKR based surrogate for the objective approximations. In order to verify the proposed methodology, a comprehensive number of data are considered from the past literature. These data have different responses ranging from three to eight (objectives). The NSGA-III is

shown to obtain good results and outperforms another recent EA. The following contributions could be concluded from this research,

- Generic objective approximation and data-driven multi-objective optimization approaches are rarely practiced together for the manufacturing process optimization, which is done in this work.
- The NSGA-III is a newly developed many-objective optimization technique, which is not yet tested for the data-driven surrogate-assisted optimization, which is done in this paper.
- The initial population generation for the data-driven EA maintains the variation in the population. For that matter, LHS techniques are mostly exploited in past. In this study, the LHS is mixed with FFD. This mixed approach incorporates more variety and proportional distribution of the solutions in the design space.
- Mostly past research on the surrogate-assisted optimization employed single surrogate based objective evaluation. In this study, the GKR, GRNN, and FFNN are utilized and compared based on the off-line data training. The best model is then selected based on the lowest MSE scores.
- The obtained solutions are confirmed with the boundary conditions and the statistical analysis proves the reliability of the EAs.

The further scope of this study is to address on-line direct optimization of the machining processes with many responses.

Acknowledgments

This work is supported by the SFI Manufacturing (Project No. 237900) and funded by the Norwegian Research Council.

References

1. Afazov, S.M. Modelling and simulation of manufacturing process chains. *CIRP J. Manuf. Sci. Technol.*, **2013**, *6*(1), 70-77.
2. Gröger, C.; Niedermann, F.; Mitschang, B. *Data Mining-driven Manufacturing Process Optimization*. Proceedings of the World Congress on Engineering, London, UK, 2012.
3. Dasgupta, D.; Michalewicz, Z. *Evolutionary algorithms in engineering applications*; Springer Science & Business Media, 2013.
4. Li, W.; Xiao, M.; Peng, X.; Garg, A.; Gao, L. A surrogate thermal modeling and parametric optimization of battery pack with air cooling for EVs, Appl. Therm. Eng., **2019**, *147*(25), 90-100.
5. Wang, H.; Jin, Y.; Jansen, J.O. Data-Driven Surrogate-Assisted Multiobjective Evolutionary Optimization of a Trauma System. *IEEE Trans. Evol. Comput.*, **2016**, *20*(6), 939-952.
6. Rajan, A.; Vijayaraghavan, V.; Ooi, M.P-L.; Garg, A.; Kuang, Y.C. simulation-based probabilistic framework for lithium-ion battery modelling. *Measurement*, **2018**, *115*, 87-94.
7. Vijayaraghavan, V.; Garg, A.; Gao, L. Fracture mechanics modelling of lithium-ion batteries under pinch torsion test. *Measurement*, **2018**, *114*, 382-389
8. Simpson, T.; Toropov, V.; Balabanov, V.; Viana, F. *Design and Analysis of Computer Experiments in Multidisciplinary Design Optimization: A Review of How Far We Have Come - Or Not*. 12th AIAA/ISSMO Multidisciplinary Analysis and Optimization Conference, Multidisciplinary Analysis Optimization Conferences, British Columbia, 2008.
9. An, Y.; Lu, W.; Cheng, W. Surrogate Model Application to the Identification of Optimal Groundwater Exploitation Scheme Based on Regression Kriging Method-A Case Study of Western Jilin Province. *Int. J. Environ. Res. Public Health*, **2015**, *12*(8), 8897-8918.
10. Messac, A. *Optimization in Practice with MATLAB*. Cambridge University Press: NY, USA, 2015.
11. Giunta, A.; Wojtkiewicz, S.; Eldred, M. *Overview of Modern Design of Experiments Methods for Computational Simulations*. 41st Aerospace Sciences Meeting and Exhibit, Aerospace Sciences Meetings, Reno, Nevada, USA, 2003.
12. Pfrommer, J.; Zimmerling, C.; Liu, J.; Kärger, L.; Henning, F.; Beyerer, J. Optimisation of manufacturing process parameters using deep neural networks as surrogate models. *Procedia CIRP*, **2018**, 72, 426-431.
13. Graning, L.; Menzel, S.; Ramsay, T.; Sendhoff, B. *Application of sensitivity analysis for an improved representation in evolutionary design optimization*. International Conference on Genetic and Evolutionary Computation, Kitakushu, Japan, 2012; 417-420.
14. Jin, Y. *Knowledge Incorporation in Evolutionary Computation*. Springer, 2005.
15. Guo, D.; Chai, T.; Ding, J; Jin, Y. Small data driven evolutionary multi-objective optimization of fused magnesium furnaces, Proceedings of IEEE Symposium Series on Computational Intelligence, 2016.
16. Jin, Y.; Wang, H.; Chugh, T.; Guo, D.; Miettinen, K. Data-Driven Evolutionary Optimization: An Overview and Case Studies. *IEEE Trans. Evol. Comput.*, **2018**, DOI: 10.1109/TEVC.2018.2869001.
17. Vijayaraghavan, V.; Castagne, S. Computational model for predicting the effect of process parameters on surface characteristics of mass finished components. Engineering Computations, **2016**, *33(3)*, 789-805.
18. Mukherjee, I.; Ray, P.K. A review of optimization techniques in metal cutting processes. *Comput. Ind. Eng.*, **2006**, *50*(1-2), 15-34.
19. Chandrasekaran, M.; Muralidhar, M.; Krishna, C.M.; Dixit, U.S. Application of soft computing techniques in machining performance prediction and optimization: a literature review. *Int. J. Adv. Manuf. Technol.*, **2010**, *46*(5-8), 445-464.
20. Cook, D.; Ragsdale, C.; Major, R. Combining a neural network with a genetic algorithm for process parameter optimization. *Eng. Appl. Artif. Intell.*, **2000**, *13*(4), 391–396.
21. Yarlagadda, P. Prediction of die casting process parameters by using an artificial neural network model for zinc alloys. *Int. J. Prod. Res.*, **2000**, *38*(1), 119-139.
22. Kolahan, F.; Liang, M. Optimization of hole-making operations: a tabu-search approach. *Int. J. Mach. Tools Manuf.*, **2000**, *40*(2), 1735-1753.
23. Chen, H.; Lin, J.; Yang, Y.; Tsai, C. Optimization of wire electrical discharge machining for pure tungsten using a neural network integrated simulated annealing approach. *Expert Syst. Appl.*, **2010**, *37*(10), 7147-7153.
24. Asokan, P.; Saravanan, R.; Vijayakumar, K. Machining Parameters Optimisation for Turning Cylindrical Stock into a Continuous Finished Profile Using Genetic Algorithm (GA) and Simulated Annealing (SA). *Int. J. Adv. Manuf. Technol.*, **2003**, *21*, 1-9.
25. Vijayakumar, K.; Prabhaharan, G.; Asokan, P.; Saravanan, R. Optimization of multi-pass turning operations using ant colony system. Int. J. Mach. Tools Manuf., **2003**, *43*(15), 1633-1639.
26. Shen, C.; Wang, L.; Li, Q. Optimization of injection molding process parameters using combination of artificial neural network and genetic algorithm method. *J. Mater. Process. Technol.*, **2007**, *183*(2), 412–418.
27. Zhou, J.; Turng, L. Process optimization of injection molding using an adaptive surrogate model with Gaussian process approach. *Polym. Eng. Sci.*, 2007, *47*(5), 684-694.
28. Ciurana, J.; Arias, G.; Ozel, T. Neural Network Modeling and Particle Swarm Optimization (PSO) of Process Parameters in Pulsed Laser Micromachining of Hardened AISI H13 Steel. *Mater. Manuf. Processes*, **2009**, *24*(3), 358-368.
29. Zhao, P.; Zhou, H.; Li, Y.; Li, D. Process parameters optimization of injection molding using a fast strip analysis as a surrogate model. *Int. J. Adv. Manuf. Technol.*, **2010**, *49*(9), 949–959.
30. Kadirgama, K.; Noor, M.M.; Abdalla, A.N. Response Ant Colony Optimization of End Milling Surface Roughness. *Sensors*, **2010**, 10(3), 2054-2063.
31. Shi, H.; Gao, Y.; Wang, X. Optimization of injection molding process parameters using integrated artificial neural network model and expected improvement function method. *Int. J. Adv. Manuf. Technol.*, **2010**, *48*(9-12), 955–962.
32. Dereli, T.; Filiz, I.; Baykasoglu, A. Optimizing cutting parameters in process planning of prismatic parts by using genetic algorithms. *Int. J. Prod. Res.*, **2001**, *39*(15), 3303-3328.
33. Thombansen, U.; Schuttler, J.; Auerbach, T.; Beckers, M. *Model-based self-optimization for manufacturing systems*. 17th International Conference on Concurrent Enterprising, 2011.
34. Farahnakian, M.; Razfar, M.; Moghri, M.; Asadnia, M. The selection of milling parameters by the PSO-based neural network modeling method. *Int. J. Adv. Manuf. Technol.*, **2011**, *57*, 49-60.
35. Yusup, N.; Zain, A.; Hashim, S. Evolutionary techniques in optimizing machining parameters: Review and recent applications (2007–2011). *Expert Syst. Appl.*, **2012**, 39(10), 9909-9927.
36. Šibalija, T.; Majstorovic, V. *Advanced multiresponse process optimisation: An Intelligent and Integrated Approach*, Springer, 2015; ISBN 978-3-319-19255-0.
37. Shakeri, S.; Ghassemi, A.; Hassani, M.; Hajian, A. Investigation of material removal rate and surface roughness in wire electrical discharge machining process for cementation alloy steel using artificial neural network. *Int. J. Adv. Manuf. Technol.*, **2016**, 82, 549-557.
38. Arnaiz-González, Á.; Fernández-Valdivielso, A.; Bustillo, A.; Norberto, L.; Lacalle, L.D. Using artificial neural networks for the prediction of

dimensional error on inclined surfaces manufactured by ball-end milling. *Int. J. Adv. Manuf. Technol.*, **2016**, 83(5-8), 847-859.
39. Xiang, G.; Zhang, Q. Multi-Object Optimization of Titanium Alloy Milling Process using Support Vector Machine and NSGA-II Algorithm. Int. J. Simul. Syst. Sci. Technol., **2016**, *17*(38), 35.1-35.6.
40. Zhou, J.; Ren, J.; Yao, C. Multi-objective optimization of multi-axis ball-end milling Inconel 718 via grey relational analysis coupled with RBF neural network and PSO algorithm. *Measurement*, **2017**, *102*, 271-285.
41. Khorasani, A.; Yazdi, M. Development of a dynamic surface roughness monitoring system based on artificial neural networks (ANN) in milling operation. *Int. J. Adv. Manuf. Technol.*, **2017**, *93*, 141-151.
42. Sangwan, K.; Kant, G. Optimization of Machining Parameters for Improving Energy Efficiency using Integrated Response Surface Methodology and Genetic Algorithm Approach. *Procedia CIRP*, **2017**; 61, 517-522.
43. D'Addona, D.; Ullah, A.; Matarazzo, D. Tool-wear prediction and pattern-recognition using artificial neural network and DNA-based computing. *J. Intell. Manuf.*, **2017**, *28*, 1285-1301.
44. Deb, K.; Jain, H. An Evolutionary Many-Objective Optimization Algorithm Using Reference-Point-Based Nondominated Sorting Approach, Part I: Solving Problems with Box Constraints. *IEEE Trans. Evol. Comput.*, **2014**, *18*(4), 577-601.
45. Ghosh, T. *Data for Multi-Response MPOP*. Mendeley Data, **2019**, DOI: 10.17632/yr4fdj9cph.1.
46. Specht, D. A general regression neural network. IEEE Trans. Neural Networks, **1991**, *2*(6), 568-576.
47. Chapelle, O.; Vapnik, V. *Model Selection for Support Vector Machines*. NIPS'99 Proceedings of the 12th International Conference on Neural Information Processing Systems, Denver, CO, 2000.
48. Brentan, B.; Laurain, V.; Aberkane, S. *How to Infer Prior Knowledge in Water Distribution Data-Driven Models?*. WDSA / CCWI Joint Conference 2018, Kingston, Ontario, Canada, 2018.
49. Poli, A.; Cirillo, M. On the use of the normalized mean square error in evaluating dispersion model performance. *Atmos. Environ. Part A*, **1993**, *27*(15), 2427-2434.
50. Deb, K; Agrawal, R. Simulated binary crossover for continuous search space. *Complex Syst.*, **1994**, *9*, 1-34.
51. Chankong, V.; Haimes, Y. *Multiobjective Decision Making Theory and Methodology*. New York: North-Holland, 1983. ISBN 9780486462899.
52. Kukkonen, S.; Deb, K. *Improved pruning of non-dominated solutions based on crowding distance for bi-objective optimization problems*. IEEE Congress on Evolutionary Computation (CEC), 2006.
53. Das, I.; Dennis, J.E. Normal-Boundary Intersection: A New Method for Generating the Pareto Surface in Nonlinear Multi Criteria Optimization Problems. *SIAM J. Optim.*, **1998**, *8*(3), 631-657.
54. Zhang, Q.; Li, H. MOEA/D: A Multiobjective Evolutionary Algorithm Based on Decomposition. *IEEE Trans. Evol. Comput.*, **2007**, *11*(6), 712-731.
55. Tzeng, C.J.; Lin, Y. H.Y.; Yang, K.; Jeng, M.C. Optimization of turning operations with multiple performance characteristics using the Taguchi method and Grey relational analysis. *J. Mater. Process. Technol.*, **2009**, *209*(6), 2753-2759.
56. Siddiquee, A.N.; Khan, Z.A.; Mallick, Z. Grey relational analysis coupled with principal component analysis for optimisation design of the process parameters in in-feed centreless cylindrical grinding. *Int. J. Adv. Manuf. Technol.*, **2010**, *46*(9-12), 983–992.
57. Chamoli, S.; Yu, P.; Kumar, A. Multi-response optimization of geometric and flow parameters in a heat exchanger tube with perforated disk inserts by Taguchi grey relational analysis. *Appl. Therm. Eng.*, **2016**, *103*, 1339-1350.
58. Armağan, M.; Arici, A. Cutting performance of glass-vinyl ester composite by abrasive water jet. *Mater. Manuf. Processes*, **2017**, *32*(15), 1715-1722.
59. Kuram, E.; Ozcelik, B. Multi-objective optimization using Taguchi based grey relational analysis for micro-milling of Al 7075 material with ball nose end mill. *Measurement*, **2013**, *46*(6), 1849-1864.
60. Kumar, Y.; Singh, H. Multi-response Optimization in Dry Turning Process Using Taguchi's Approach and Utility Concept. *Procedia Mater. Sci.*, **2014**, *5*, 2142-2151.
61. Chen, H.; Chang, S.; Tang, C. Application of the Taguchi Method for Optimizing the Process Parameters of Producing Lightweight Aggregates by Incorporating Tile Grinding Sludge with Reservoir Sediments. *Materials (Basel)*, **2017**, *10*(11), E1294.
62. Vellaiyan, S.; Amirthagadeswaran, K. Taguchi-Grey relational-based multi-response optimization of the water-in-diesel emulsification process. *J. Mech. Sci. Technol.*, **2016**, *30*, 1399-1404.
63. Krishnamoorthy, A.; Boopathy, S.; Palanikumar, K.; Davim, J. Application of grey fuzzy logic for the optimization of drilling parameters for CFRP composites with multiple performance characteristics. *Measurement*, **2012**, *45*(5), 1286-1296.
64. Sahu, P.; Pal, S. Multi-response optimization of process parameters in friction stir welded AM20 magnesium alloy by Taguchi grey relational analysis. *J. Magnesium Alloys*, **2015**, *3*(1), 36-46.
65. Stein, M. Large Sample Properties of Simulations Using Latin Hypercube Sampling. *Technometrics*, **1987**, *29*(2), 143-151.
66. Zitzler, E. *Evolutionary Algorithms for Multiobjective Optimization: Methods and Applications*. Ph.D. Thesis, ETH Zürich, Zürich, 1999.